Available at www.sciencedirect.com

ScienceDirect

journal homepage: www.elsevier.com/locate/watres

Phototransformation of selected human-used macrolides in surface water: Kinetics, model predictions and degradation pathways

Davide Vione[b], *Juliana Feitosa-Felizzola*[a], *Claudio Minero*[b], *Serge Chiron*[a,*]

[a]*Laboratoire Chimie Provence, Aix-Marseille Universités-CNRS (UMR 6264), 3 place Victor Hugo, 13331 Marseille cedex 3, France*
[b]*Dipartimento di Chimica Analitica, Università di Torino, Via Pietro Giuria 5, 10125 Torino, Italy*

ARTICLE INFO

Article history:
Received 25 September 2008
Received in revised form
9 January 2009
Accepted 25 January 2009
Published online 6 February 2009

Keywords:
Macrolides
Phototransformation
Surface waters
Model prediction
By-products

ABSTRACT

The phototransformation of clarithromycin and roxithromycin, two human-used macrolide (MLs) antibiotics was investigated in surface waters. Photolysis kinetic data suggest that degradation in water would occur via the direct photolysis of the Fe(III)–MLs complexes. Hydroxyl radicals, singlet oxygen and other photooxidants generated from nitrate ions and from excited chromophores present in humic acids appeared to have only a very limited impact on the overall degradation of MLs under the adopted UV–vis irradiation conditions. A photolysis model applied to the Fe(III)–clarithromycin complex in river water showed that a half-life of 40 days was predicted under clear-sky irradiation in November, 26 days in February, and 10 in May. Direct photolysis could have a limited impact on the environmental concentrations of MLs in rivers, due to a too short water residence time but might be important in shallow lakes and lagoons. Photoinduced degradation of MLs mainly implied changes in the structure of the aglycone, probably leading to their detoxification because the pseudoerythromycin derivatives have very little antimicrobial activity.

1. Introduction

Macrolides (MLs) are the second most important antibacterial agents used for human therapy after the β-lactam family. In 2004, the most used MLs in human medicine in France have been erythromycin A (27,042 kg), clarithromycin (15,015 kg), josamycin (12,802 kg), and to a lesser extent azithromycin (4073 kg) and roxithromycin (3404 kg) (Knappe EU project, 2008). MLs consist of a 14- to 16-carbon lactone ring, which is substituted with hydroxyl, alkyl and ketone groups as well as neutral and amino sugars bound to the nucleus through ether linkages (Pal, 2006). The biochemical activity of MLs is believed to be derived from inhibition of protein synthesis via specific hydrogen bonding in the peptidyl transferase cavity of bacterial 23S rRNA (Schlünzen et al., 2001). Biological activity is mainly related to the presence of the tert-amino sugar and the hydroxyl groups located on the lactone ring. The presence of the neutral sugar at the C-3 position of the ring is not fully required (Pal, 2006).

MLs have been frequently detected worldwide in the final effluents of wastewater treatment plants (WWTPs, Gros et al., 2007; Miao et al., 2004), in surface waters at concentration levels of 1–250 ng/L (Calamari et al., 2003; Managaki et al., 2007), and even in drinking water at low ng/L levels (Ye et al., 2007). Significantly higher concentrations of MLs have been detected in river sediments, indicating the possible

* *Corresponding author*. Tel.: +33 4 91 10 85 25; fax: +33 4 91 10 63 77.
E-mail address: serge.chiron@up.univ-mrs.fr (S. Chiron).
URL: http://www.chimicadellambiente.unito.it
0043-1354/$ – see front matter © 2009 Elsevier Ltd. All rights reserved.
doi:10.1016/j.watres.2009.01.027

accumulation of MLs in that compartment (Kim and Carlson, 2007). Concerns on MLs residues in the environment arise from their high toxicity toward green algae (Isidori et al., 2005), their possible high persistence in surface waters (McArdell et al., 2003), their known ability to enzymatically inhibit the cytochrome P-450 (Masubuchi and Horie, 2007), and their possible contribution to the selection of antibiotic-resistant bacterial strains, in a similar way as other antibiotic classes (Pei et al., 2007). Consequently, CLA has been classified as a priority human pharmaceutical to be monitored in French surface waters (Besse and Garric, 2008).

To refine the environmental risk assessment of human-used MLs in surface waters, the significance of natural attenuation processes such as photodegradation has to be assessed. Differently from other antimicrobial agents such as fluoroquinolones (Belden et al., 2007), tetracyclines (Werner et al., 2006) and sulphonamides (Boreen et al., 2004), little is known in this field for MLs. Unlike tylosin, a widely used veterinary macrolide antibiotic exhibiting a conjugated diene moiety (Werner et al., 2007), human-used MLs do not absorb light at $\lambda > 290$ nm, which excludes any direct photochemistry. However, it has been observed that they undergo electronic interactions with transition metals such as Fe(II), Cu(II) and Zn(II) (Hamdan, 2003). The iron(III)–MLs complex, which are believed to be the most important photochemically active species (Kari and Giger, 1995) might be relevant for the degradation of MLs in surface waters. Neither the implications of MLs speciation nor the impact of indirect photolysis on MLs photochemical fate in surface waters have been investigated yet. Consequently, the contribution of this work will be to investigate the implication of phototransformation processes of human-used MLs in surface waters by taking clarithromycin (CLA) and roxithromycin (ROX) as probe compounds. The structures of CLA and ROX are given in Fig. 1. Laboratory-scale experiments were conducted to describe the phototransformation kinetics of MLs. Predicted half lives were calculated by means of a photolysis model, and tentative transformation reaction schemes are proposed on the basis of the identification of the major by-products.

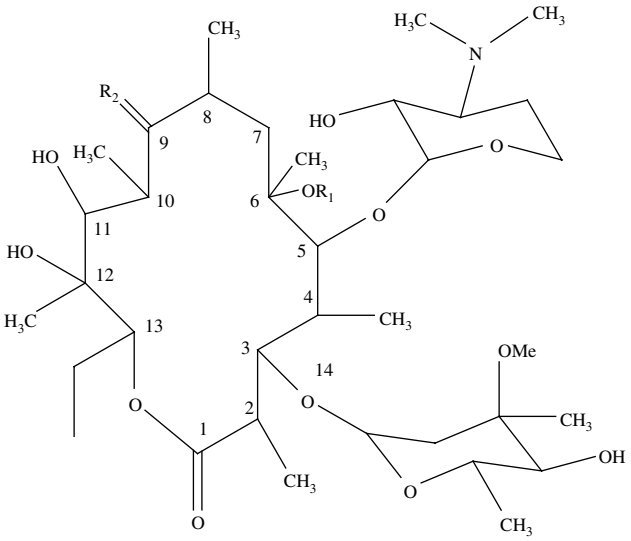

Roxithromycin: R_1 = H; R_2 = $NOCH_2OCH_2CH_2OCH_3$
Clarithromycin: R_1 = CH_3; R_2 = O

Fig. 1 – Structures of the macrolides investigated in this study.

2. Experimental

2.1. Chemicals and materials

Clarithromycin (purity >95%), roxithromycin (>90%), NaCl (>99%), $NaNO_3$ (>99%), $FeCl_3 \cdot 6H_2O$ (>97%), ortho-phenant hroline (>99%) and humic acid sodium salt, technical grade (iron-free) were purchased from Sigma–Aldrich (St Quentin Fallavier, France). Methanol and acetonitrile (Lichrosolv gradient grade) were from VWR Int. Water was purified with a MilliQ sytem (Millipore, Milford, MA, USA).

2.2. Speciation studies

The complexation equilibrium between MLs and Fe(III) ions was studied by UV–vis absorption spectroscopy. This series of experiments was carried out in 50:50 vol/vol methanol–water to achieve a sufficient solubility of the iron(III)–MLs complexes. Iron(III) solutions were prepared from $FeCl_3 \cdot 6H_2O$. These solutions were standardised by titration with EDTA using variamine blue indicator. Solutions of the required pH 7 ± 0.2 were obtained using 1 M NaOH. All solutions were adjusted to an ionic strength of 0.01 M with sodium chloride. The design of the experiments was based on the mole ratio method, where a series of test tubes containing a fixed concentration of Fe(III) at 4.46×10^{-5} M and increasing concentrations of MLs were prepared so that the mole ratio (r) of MLs to metal was in the 0–50 range. After standing for 1 h above 20 °C to ensure completion of the complex formation, UV–visible data were obtained by using an HP 8543A diode-array spectrophotometer and by using methanol–water (50:50) as a blank. All the experiments were repeated three times and the data were averaged. The dissociation constant, K_d, for the iron(III)–macrolide complexes was measured according to the conventional Scott equation (Li and Purdy, 1992).

$$[ML_0][Fe_0^{3+}]/\Delta_{Abs} = K_d/\Delta\varepsilon + ([ML_0] + [Fe_0^{3+}])/\Delta\varepsilon$$

where $[ML_0]$ is the total concentration of macrolide, $[Fe_0^{3+}]$ is the total concentration of iron(III), $\Delta\varepsilon$ is the difference of the molar absorption coefficients for free and complexed iron(III), and Δ_{Abs} is the change in absorbance upon addition of the macrolide. The data were treated by plotting $[ML_0][Fe_0^{3+}]/\Delta_{Abs}$ vs. $([ML_0] + [Fe_0^{3+}])$, providing a slope of $1/\Delta\varepsilon$ and an intercept of $K_d/\Delta\varepsilon$.

2.3. Phototransformation kinetics

Initial MLs concentrations (1.34×10^{-6} M) below published water solubility and Fe(III) concentrations of 37.7 μM were used. The experiments were carried out with a 0.5 L cylindrical immersion-type photo-reactor (Heraeus TQ 150 model) equipped with a water-cooled, medium-pressure mercury lamp with maximum emission wavelengths at 313, 366, 406, 436, 546, and 578 nm. The radiation path length inside the

reactor was 2 cm. The reactor was made of Pyrex glass in order to cut off the wavelengths shorter than 290 nm. The whole assembly was mounted on a magnetic stirrer and wrapped with aluminium foil. Aliquots of 10 mL were analysed at selected intervals after a filtration step through 0.45 μm filter membranes (cellulose acetate, Millipore). In order to avoid losses of MLs due to sorption on glassware surfaces, the reactor was silanised. The silanised glass reactor was prepared by treating the reactor with 5% dimethyldichlorosilane in toluene, followed by rinsing with toluene and methanol to remove the residual silanising agent. Finally the reactor was rinsed with deionised water and dried before use. The hazardous process was carried out in a hood with chemicals and glassware handled with double gloving. *Ortho*-phenanthroline was used to test for the presence of Fe^{2+} ions in solutions containing Fe^{3+} as recommended by Wong-Wah-Chung et al. (2006). The absorbance at 525 nm, which is the λ_{max} for the Fe^{2+}–phenanthroline complex was recorded, and Fe^{2+} ion concentrations were calculated by using a molar absorption coefficient of $1.1 \times 10^4\ M^{-1}\ cm^{-1}$. The limit of detection of the method was 1×10^{-6} M.

2.4. Natural water irradiation experiments

River water samples were collected at the River Arc (Southern France), which is a small Mediterranean river flowing into a densely populated area. Samples were taken from bridges at the centroid of flow, approximately 20 cm below the surface of the water, using LDPE plastic bottles, and were immediately transferred to glass bottles and stored at 4 °C (DOC = 25 ± 0.9 mg/L; pH 7.6; $[NO_3^-] = 9 \pm 0.5$ mg/L; $[SO_4^{2-}] = 36 \pm 1.5$ mg/L; $[Cl^-] = 88 \pm 1.2$ mg/L). Filtered Fe concentrations in the River Arc were in the 8–12 μM range. Water samples were filtered using 0.45 μm glass filters (Waters, Milford, MA) and analysed within the same day according to a previously validated analytical procedure in our Lab, and based on on-line SPE coupled to LC and tandem mass spectrometry (Feitosa-Felizzola et al., 2007). Limits of quantification (LOQs) of the analytical method were 4 ± 0.3 and 54 ± 4.3 ng/L for CLA and ROX, respectively. In order to distinguish the photolabile fraction from total MLs species, we have developed the following procedure. An aliquot of a real river water sample was analysed for total MLs content; another one was analysed after irradiation under a medium-pressure mercury lamp ($\lambda > 290$ nm) for 8 h. The fraction of photolabile Fe(III)–MLs species was calculated by subtracting the MLs concentration after irradiation from the total concentration of MLs in the original sample.

2.5. Instrumental analysis

The time trend of MLs degradation was monitored by liquid chromatography coupled to mass spectrometry (LC/MS) in the selective reaction monitoring (SRM) mode of acquisition. HPLC analyses were performed with an Elite LabChrom high-pressure binary pump (VWR-Hitachi, Fontenay, France). A Beta-Basic 150 × 2 mm C-18 endcapped column (3 μm particle size) was used. The mobile phase consisted of 60% A (water + 0.1% HCOOH) and 40% B (acetonitrile). An isocratic mode of elution was adopted at a flow rate of 0.2 mL/min. The Esquire 6000 ion trap mass spectrometer (Bruker Daltonic, Bremen, Germany) was equipped with an electrospray (ESI) source operated in positive polarity. Operating conditions of the source were: capillary voltage, 4000 V; nebuliser pressure, 45 psi; drying gas flow, 10 L/min at a temperature of 365 °C. Selected transitions were 748 > 590 and 837 > 679 for CLA and ROX, respectively. Limits of detection were below 0.01 mg/L with an injection volume of 20 μL. For by-product identification, a binary gradient was adopted. The initial conditions were 90% A and 10% B. The mixture was ramped linearly to 10% A and 90% B at 30 min, held for 5 min and then back to initial conditions in 5 min. Tentative structural assignments for transformation products were made on the basis of their MS-MS^3 mass fragmentation patterns, and by comparing the MS spectra with those already published in the literature.

3. Results and discussion

3.1. Speciation studies with iron

Although the investigated MLs undergo interaction with different transition metals such as Cu, Zn, Fe (Hamdan, 2003), only Fe(III)–MLs were taken into account because the complexes of organic ligands with Fe(III) are the most important photochemically active species in the vast majority of cases, also because of the more elevated concentration of Fe(III) compared to other metals (Kari and Giger, 1995). Accordingly, Fe(III)–MLs are potentially relevant for the photochemical degradation of MLs in surface waters. Spectrophotometric titrations showed that CLA and ROX act as ligands in the presence of iron(III). The overlaid UV spectra of $FeCl_3$ titrated with MLs in methanol:water (50/50) are reported in Fig. 2 for CLA and Fig. S1 (Supplementary material) for ROX. They show a shift of the absorption band at $\lambda_{max} = 361$ nm to longer wavelengths (3–5 nm), along with an increase of the absorption intensity as the drug-to-metal ratio *r* increased from 0 to 50. This increase in absorbance was attributed to formation of complex between Fe(III) and the MLs. A unique isosbestic point, observed at 300 nm, indicates the presence of a single complex. Application of the Scott equation (see inset in Fig. 2 for CLA and in Fig. S1 for ROX) allowed the determination of the formation constant K_d of the complex. A plot of the data in the form of $[ML_0][Fe_0^{3+}]/\Delta_{Abs}$ vs. $([ML_0] + [Fe_0^{3+}])$ showed linear correlation, indicating Fe + ML ⇄ Fe–ML equilibrium model (stoichiometry 1:1), and providing a slope of $1/\Delta\varepsilon$ and an intercept of $K_d/\Delta\varepsilon$. Accordingly, the complex formation constant values were found to be $7.43 \pm 1.18 \times 10^3\ M^{-1}$ and $6.80 \pm 1.22 \times 10^3\ M^{-1}$ for CLA and ROX, respectively. It was not possible to elucidate the chelating sites, but it has been reported that the complex formation between MLs and monovalent cations involves several oxygen atoms of the lactone ring (Gierczyk et al., 2005).

3.2. Photodegradation kinetics

In dark controls, MLs hydrolysis rates in the presence of iron(III) were low with half lives calculated as 1.99 ± 0.1 and 2.67 ± 0.15 d for ROX and CLA, respectively. In contrast, in the presence of light a clear photoinduced transformation of

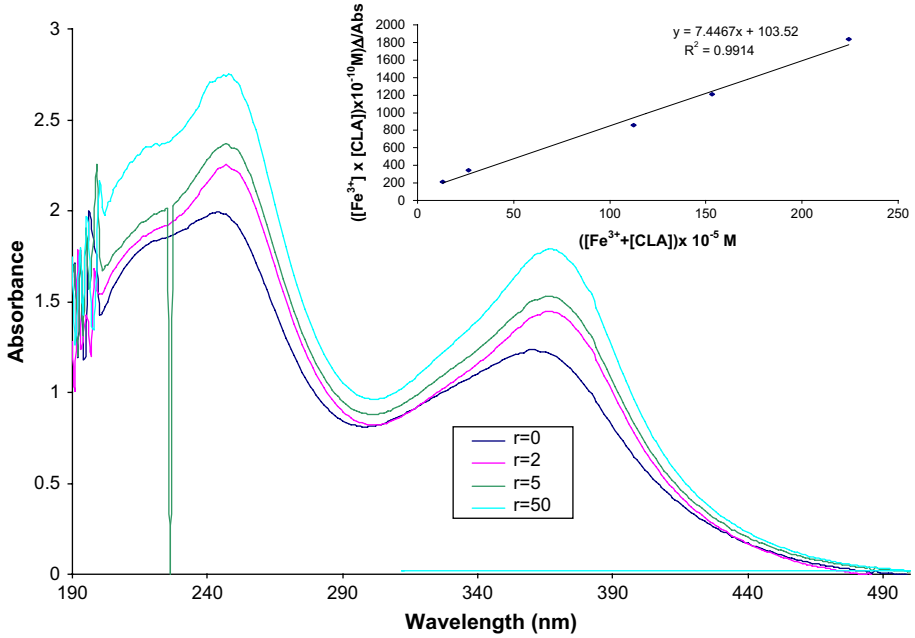

Fig. 2 – Overlaid UV spectra of $FeCl_3$ titrated with Clarithromycin. $[Fe^{3+}] = 4.46\ 10^{-5}$ M; *r* is the mole ratio of ML to metal; solvent methanol:water (50:50, v/v); pH 7. Plots of the data in the form of the Scott equation in inset.

investigated MLs with iron(III) was observed. Fig. 3 shows the photodegradation rate constant of investigated MLs (initial concentration $[ML]_0 = 1.34\ \mu M$) under UV–vis irradiation and under different experimental conditions at pH 7 ± 0.2: in the presence of iron(III) ($[Fe^{3+}] = 37.7\ \mu M$); nitrate ions ($[NO_3^-] = 0.8 \times 10^{-3}$ M), or dissolved organic matter ([DOM] = 10 mg/L). These concentrations were selected because they are relevant for environmental conditions. Our experimental results for ROX and CLA were well fitted by the first-order kinetic model, and it is apparent from Fig. 3 that the photodegradation rate constants were by far the highest in the presence of Fe(III)

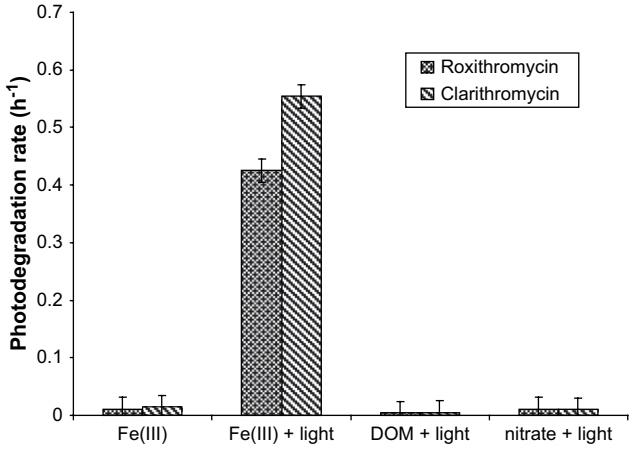

Fig. 3 – Photodegradation rate constant (h^{-1}) of human-used macrolides under UV–vis lamp irradiation and different experimental conditions. $[ML]_0 = 1.34\ \mu M$; $[Fe^{3+}] = 37.7\ \mu M$; $[NO_3^-] = 0.8 \times 10^{-3}$ M; [DOM] = 10 mg/L (humic acids); pH 7.

under irradiation. Under these conditions, half lives of 1.25 ± 0.06 h and 1.63 ± 0.10 h for CLA and ROX were measured, respectively. The apparent reaction rate constants are within the same order for CLA and ROX, indicating that both chemicals reacted at fairly comparable rates. Hydroxyl radicals, singlet oxygen and other photooxidants generated from nitrate ions and from excited chromophores present in humic acids appeared to have only a very limited impact on the overall degradation of MLs. These findings suggest that photodegradation with Fe(III) involves the Fe(III)–MLs complexes and not ·OH photogenerated by Fe(III). Interestingly, the bimolecular reaction rate constant between the protonated form of ROX and hydroxyl radicals was previously quantified at a value around $5 \times 10^9\ M^{-1}\ s^{-1}$ (Dodd et al., 2006). This high reactivity is typical for the reaction of many substrates with ·OH. From previous studies carried out under the same lamp it is possible to derive that the formation rate of ·OH with 0.8 mM nitrate would be an order of magnitude higher compared to 37.7 μM Fe(III) (Chiron et al., 2006). Changes in lamp intensity over time could modify the absolute rates of ·OH photogeneration by the two species, but their ratio would remain about the same. In the studied systems ($ROX + NO_3^-$, ROX + Fe(III)), ROX would be the only important scavenger of ·OH. The degradation rate of ROX because of reaction with ·OH would therefore be equal to the generation rate of the hydroxyl radical, independently of the reaction rate constant between the different species of ROX and ·OH. As a consequence, the degradation rate of ROX because of ·OH produced by 37.7 μM Fe(III) would be about one tenth of the rate of ROX degradation induced by 0.8 mM nitrate. Based on the above considerations, a pseudo-first order degradation rate constant of around $0.1 \times 0.01\ h^{-1} = 10^{-3}\ h^{-1}$ can be assumed for the reaction between ·OH and 1.34 μM ROX in the presence of Fe(III). The actual degradation rate constant of

ROX upon irradiation with Fe(III) is over 400 times higher (see Fig. 3). It can therefore be concluded that the degradation of ROX takes place upon photolysis of a Fe(III)–ROX complex, and to a negligible extent for reaction with photogenerated $^{\bullet}OH$. Additionally, the photolysis rates of ROX in spiked natural waters from the River Arc matched the photodegradation rates in deionised water plus Fe(III). The DOM contained in river water would be able to scavenge $^{\bullet}OH$ at a considerable extent, and an $^{\bullet}OH$-initiated degradation process should show different kinetics in natural samples or in synthetic solutions. In contrast, important differences between natural and synthetic systems are not expected in the case of the photolysis of Fe^{3+}–ROX, which is therefore a more likely explanation for the degradation of ROX.

The knowledge of the fraction of MLs present as iron(III) complexes in river water is required to understand the photochemical fate of MLs. This fraction is referred as the photolabile MLs for practical reasons because Fe(III)–MLs is the only fraction of macrolide that is degraded in sunlight. The occurrence of such a photolabile fraction can be reasonably assumed because CLA, for instance, associates with dissolved humic acids with association constants similar in magnitude ($10^{3.9}$–$10^{4.6}$) to those of many nonpolar contaminants (Sibley and Pedersen, 2008). Consequently, after degradation of the photolabile MLs species (mostly Fe(III)–MLs complexes), the formation of additional Fe(III)–macrolide complexes is not expected and the photostable ones could remain in the water body. The Fe(III)–CLA fraction was assessed by an indirect method, in which photolabile CLA was selectively degraded by UV–vis irradiation. Accordingly, water samples contaminated by CLA were collected from the Arc River. CLA concentrations were determined before and after irradiation (8 h). Chromatograms corresponding to the analysis of a typical river water sample are provided as Supplementary material (Fig. S2). After 8 h irradiation, an average decrease of 45% in the concentration of CLA was recorded, suggesting that photodegradable Fe(III)–CLA might account approximately for half of the CLA species in surface waters. Predictions of thermodynamic equilibrium calculations (around 10% by setting concentrations of Fe(III) and CLA at 1 mg/L and 1 μg/L, respectively) are in contradiction to the high fraction of photolabile CLA in surface water (around 50%). Assuming that Fe(III)–CLA complexes are formed in WWTPs where iron is used for phosphate precipitation, irradiation experiments show that chemical equilibrium is not reached in river water. A likely reason is kinetic limitations of the metal-exchange processes, which allow the survival of the complex in river water and which were previously reported for Fe(III)–EDTA complexes (Xue et al., 1995).

3.3. *Photodegradation pathways in the presence of Fe(III)*

Photodegradation of CLA with Fe(III) produced three major by-products designated as C1, C2 and C3, as determined by LC/MS (Fig. 4a). Analysis of C3 produced a mass spectrum with a molecular ion $[M+H]^+$ at *m/z* 764.5. The MS^2 spectrum of C3 (Fig. S3, Supplementary material) was characterised by a base peak at *m/z* 606.5, corresponding to losses of the cladinosyl moiety. The product ion at *m/z* 158 was assigned to the desosamine sugar because that moiety contains an ionisable amino function. The lack of the product ion at *m/z* 365 in the MS^3 spectrum of C3, using the ion at *m/z* 606.5 as precursor ion (Fig. S4, Supplementary material), revealed that the lactone ring was modified. The presence of the ion at *m/z* 365 gives in fact information on the integrity of the aglycone structure (Leonard et al., 2006). The product ions at *m/z* 570, 538 and 574 could easily be explained by losses of H_2O and methanol. The other product ions at *m/z* 399 and *m/z* 307 could not be identified properly. MS analysis of C2 with a molecular ion $[M+H]^+$ at *m/z* 748.5, the same as CLA, possibly indicated rearrangement. Finally, the MS/MS spectrum of C1 was characterised by a molecular ion $[M+H]^+$ at *m/z* 622.5 and a fragment ion at *m/z* 158. On the basis of the MS fragmentation patterns alone, a definitive assignment of a structure to C1–C3 was not possible. To get more insights into the mechanisms of CLA degradation, unfiltered solutions were treated by *ortho*-phen anthroline to measure the total Fe(II) concentration in the system. The occurrence of Fe(II) at $t=0$ ($[Fe(II)]_0 = 3\times10^{-6}$ M) might be attributed to a thermal redox process between ML and Fe(III). Then, the concentration of Fe(II) increased with irradiation time to reach a plateau at $[Fe(II)] = 5\times10^{-5}$ M, suggesting that the redox process is enhanced in the presence of light. This finding could be consistent with a ligand-to-metal charge transfer upon radiation absorption by the complex Fe^{3+}–CLA.

The number of transferred electrons was lower than one per molecule of CLA, probably because in oxygenated solution Fe(II) was reoxidised into Fe(III) at circumneutral pH (Pham and Waite, 2008). That would hinder an accurate quantification of Fe(II). Moreover, the concentration of C1–C3 was assessed assuming that the MS response of C1, C2 and C3 was identical to that of CLA. This method indicated (results not reported) that CLA was first transformed into C3, followed by the concurrent transformation of C3 into C2 and C1. C2 accounted for approximately 75% of the initial concentration of CLA after complete CLA degradation. On the basis of these experimental results and of the MS^n data, a tentative phototransformation pathway of CLA in water in the presence of Fe(III) was proposed (Fig. 5). Note that the transformation of CLA into C3, involving the cleavage of the lactone ring, also requires an oxidation step to yield the carbonyl group in the position corresponding to the C-13 of CLA. A likely scenario for such an oxidative cleavage is the formation of ion dipole and coordination interactions between the carbonyl group (C-1) of the lactone and a Fe(III) ion. These interactions would result in the formation of an oxygen-to-metal ligand bond (e.g. $O\cdots Fe^{3+}$), and would provide a partial single-bond character to the carbonyl group(s) of CLA. The H_2O or OH^- nucleophilic attack and the hydrolysis of the lactone ring would therefore be easier. The hydrolysis pathway is probably started by a ligand-to-metal charge transfer as depicted in Fig. 6, leading to the oxidation of the position C-13 to a ketone function. The photoinduced transfer of one electron from CLA to Fe^{3+} would yield Fe^{2+} as observed, and the positively charged ring would be more exposed to the following nucleophilic attack.

The transformation of C3 into C2 is likely due to a translactonisation reaction between the 11-OH and the lactone group, as already reported for ERY-A (Kibwage et al., 1987). C1 might result from the hydrolysis of the second carbonyl group

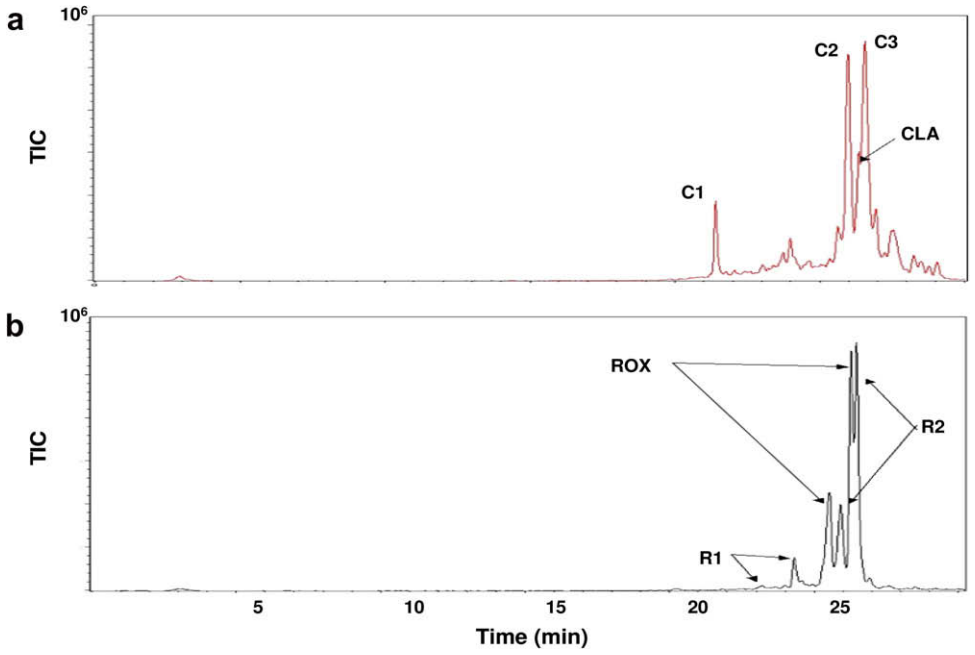

Fig. 4 – Typical total ion chromatograms (TIC) showing the separation a) of three photoproducts of clarithromycin, C1, C2 and C3 and b) of two photoproducts of roxithromycin, R1 and R2.

of CLA at the C-9 position, giving a compound of MW = 621.5. The process could follow a similar pathway as already proposed for the hydrolysis of the lactone function.

ROX eluted as two peaks (Fig. 4b). The second compound exhibited the same MW as ROX, and is likely to be an isomer: isomerisation of ROX to its Z-isomer has in fact been reported (Ye et al., 2007). Photodegradation of ROX with Fe(III) produced a major by-product (R2) and a minor one (R1) as depicted in Fig. 4b. With a molecular weight of 853.6 (16 mass units higher than that of ROX), R2 probably resulted from the cleavage of the lactone function in a similar way as CLA. MS data for R2 are provided as Supplementary material (Figs. S5, S6).

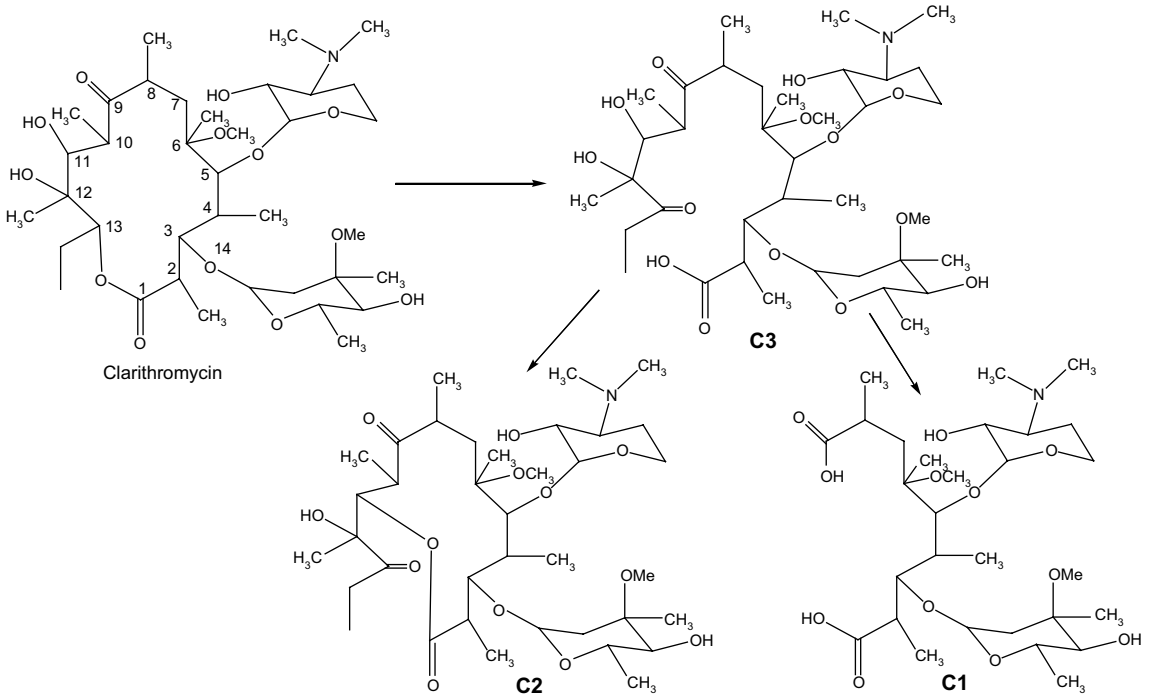

Fig. 5 – Possible phototransformation pathways of clarithromycin in water in the presence of Fe(III), under UV–vis lamp irradiation.

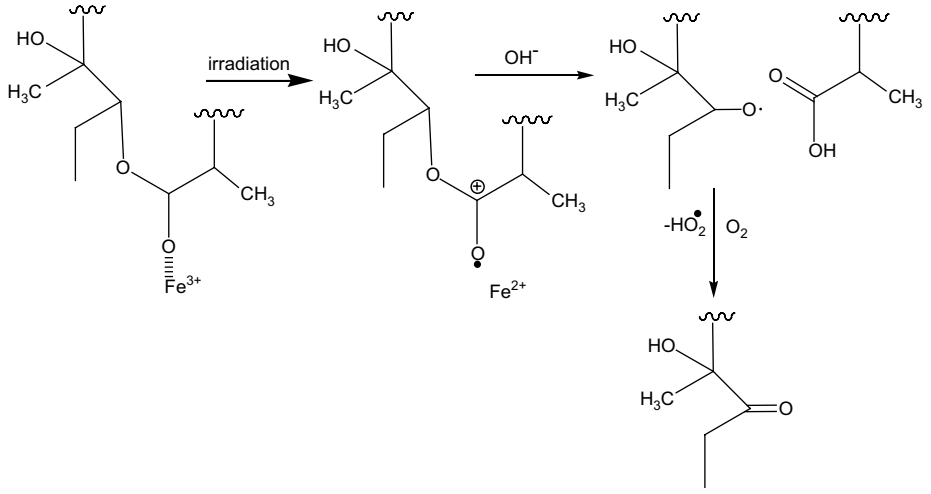

Fig. 6 – Mechanism of cleavage of the lactone ring in the presence of Fe(III) and under UV–vis lamp irradiation.

Surprisingly, translactonisation was not observed for ROX, probably because the 11-OH group is engaged in hydrogen bonding with the oxygen (19-O–Me, 17-OCH_2) of the 9-[O-(2,5-dioxahexyl)oxime] chain (Gharbi-Benarous et al., 1991). ROX underwent also slow losses of the cladinose sugar to give R1, identified as 3-O-decladinosyl-roxithromycin by comparison of its MS/MS spectrum with available data in the literature. A tentative phototransformation scheme of ROX in the presence of Fe(III) is provided in Supplementary material (Fig. S7).

In contrast to dark reactivity that mainly leads to the hydrolysis of the cladinose sugar (Pal, 2006), the photoinduced degradation of CLA and ROX implies changes in the structure of the aglycone. Such a degradation pathway probably leads to MLs detoxification, because the pseudoerythromycin derivatives (C2 and R2) have very little antimicrobial activity (Kidwage et al., 1987).

3.4. *Model predictions*

Laboratory data were extrapolated to the water column of the Arc River in the case of CLA, using a direct photolysis model. The optical properties and the photochemistry of the Fe(III)/clarithromycin (CLA) system were studied to derive the absorption spectrum of Fe^{3+}–CLA and its photolysis quantum yield, and to enable the modelling of the half-life time of the complex in river water due to the direct photolysis. The preliminary steps (spectrum of the Fe^{3+}–CLA complex and calculation of its average photolysis quantum yield in the 300–450 nm interval, $\phi_{Fe-CLA} = 5.8 \times 10^{-5}$) are described in Supplementary material.

Fig. 7 reports the molar absorption coefficient of Fe^{3+}–CLA and the absorption spectrum of river water for an optical path length $b = 1$ cm, together with the emission spectrum $P_o(\lambda)$ of sunlight under summertime irradiation conditions (clear sky, noon, mid-latitude; Frank and Klöpffer, 1988). Such conditions, corresponding to a sunlight UV irradiance of 30 W m^{-2} are relevant to the case of Southern France at the end of May, but will also be scaled for the actual diurnal variation of sunlight intensity.

The wavelength interval to be considered is that from 300 to 480 nm, where sunlight absorption by the complex Fe^{3+}–CLA is operational. The overall photon flux absorbed by river water in that interval is (in einstein cm^{-2} s^{-1}):

$$P_a^{tot} = \int_{\lambda=300\ nm}^{\lambda=480\ nm} P_o(\lambda) \cdot \left(1 - 10^{-A(\lambda)\cdot d}\right) d\lambda \quad (1)$$

where if $A(\lambda)$ is the absorbance of river water for $b = 1$ cm, d is the average depth of the water column in cm. It is possible to define the absorption fraction of river water, $f_{tot} = P_a^{tot} \cdot [\int_{\lambda=300\ nm}^{\lambda=480\ nm} P_o(\lambda) d\lambda]^{-1}$, and its total absorbance $A_{tot} = -\log_{10}(1 - f_{tot})$ (Braslavsky, 2007). If one considers the actual water column depth $d = 50$ cm, the results of the numerical integration of equation (1) give $f_{tot} \approx 1$, and $A_{tot} \to \infty$ as a consequence. To enable numerical integration it is better to consider $d = 10$ cm, giving $P_a^{tot} = 2.96 \times 10^{-8}$ einstein cm^{-2} s^{-1}, $f_{tot} = 0.96$, and $A_{tot} = 1.36$. Under the same water column depth ($d = 10$ cm) it is possible to calculate the absorbed photon flux P_a^{Fe-CLA} of the complex Fe^{3+}–CLA, in the

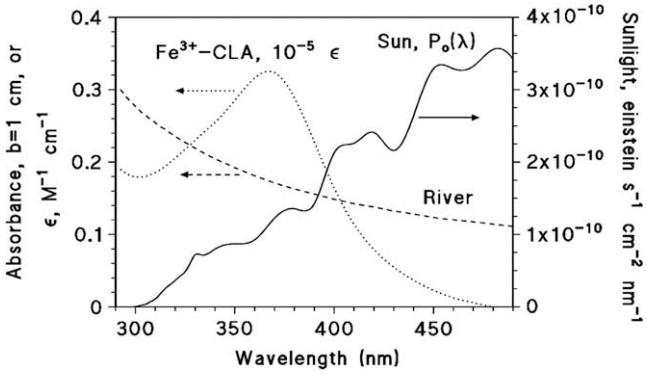

Fig. 7 – Molar absorption coefficient of Fe^{3+}–CLA, absorption spectrum of river water for an optical path length $b = 1$ cm, and emission spectrum $P_o(\lambda)$ of sunlight under summertime irradiation conditions (clear sky, noon, mid-latitude; Frank and Klöpffer, 1988).

case it were the only absorbing species in the system, as follows:

$$P_a^{Fe\text{–}CLA} = \int_{\lambda=300\ nm}^{\lambda=480\ nm} P_o(\lambda)\cdot\left(1-10^{-[\varepsilon Fe\text{–}CLA(\lambda)]\cdot d\cdot[Fe\text{–}CLA]}\right)d\lambda \quad (2)$$

In the water of the River Arc it was found [Fe^{3+}–CLA] = 6.7×10^{-7} M, and $\varepsilon_{Fe\text{–}CLA}(\lambda)$ is reported in Fig. 7. The numerical integration yields $P_a^{Fe\text{–}CLA} = 4.29\times10^{-9}$ einstein $cm^{-2}\,s^{-1}$, from which $f_{Fe\text{–}CLA} = 0.14$ and $A_{Fe\text{–}CLA} = 0.065$. The most important values obtained so far are $A_{tot} = 1.36$ and $A_{Fe\text{–}CLA} = 0.065$, and even more their ratio $A_{Fe\text{–}CLA}\cdot A_{tot}^{-1} = 0.48$. The absorbance of Fe^{3+}–CLA would be the same when the complex is alone in solution and when it is in river water. Moreover, because the absorbance values are proportional to the optical path length, the ratio $A_{Fe\text{–}CLA}\cdot A_{tot}^{-1}$ would not vary for a water column depth of 10 or 50 cm. For $d = 50$ cm, according to equation (1) the absorbed photon flux of river water would be $P_a^{tot} = 3.1\times10^{-8}$ einstein $cm^{-2}\,s^{-1}$. The ratios between the absorbance values of different species in a mixture are the same as the ratios between the absorbed photon fluxes (Braslavsky, 2007). Accordingly, the absorbed photon flux of 6.7×10^{-7} M Fe^{3+}–CLA would be $P_a^{Fe\text{–}CLA} = P_a^{tot}\cdot A_{Fe\text{–}CLA}\cdot A_{tot}^{-1} = 1.5\times10^{-9}$ einstein $cm^{-2}\,s^{-1}$, valid for 30 W m^{-2} sunlight UV irradiance.

The absorbed photon flux of Fe^{3+}–CLA can be assessed over a surface of 1 cm^2, which for a column depth of 50 cm means a volume of 50 cm^3 = 0.05 L. The volumetric photon flux absorbed by 6.7×10^{-7} M Fe^{3+}–CLA in river water would be $(P_a^{Fe\text{–}CLA})_V = P_a^{Fe\text{–}CLA}\cdot 0.05\ L\ cm^{-2} = 3.0\times10^{-8}$ einstein $L^{-1}\,s^{-1}$. This value, combined with an average photolysis quantum yield $\phi_{Fe\text{–}CLA} = 5.8\times10^{-5}$, gives a rate of direct photolysis $R_{Fe\text{–}CLA} = \phi_{Fe\text{–}CLA}\cdot P_a^{Fe\text{–}CLA} = 1.7\times10^{-12}$ M s^{-1}. The process of direct photolysis would usually follow a first-order kinetics, and in the initial rate approximation it would be $R_{Fe\text{–}CLA} = k_{Fe\text{–}CLA}\cdot[Fe^{3+}\text{–}CLA]$. The pseudo-first order degradation rate constant would therefore be $k_{Fe\text{–}CLA} = R_{Fe\text{–}CLA}\cdot[Fe^{3+}\text{–}CLA]^{-1} = 2.6\times10^{-6}\ s^{-1}$. From $k_{Fe\text{–}CLA}$ it is possible to obtain the half-life time for direct photolysis, $t_{1/2} = 0.693 k_{Fe\text{–}CLA}^{-1} = 2.7\times10^5$ s. Such a $t_{1/2}$ value would be observed for a constant 30 W m^{-2} sunlight UV irradiance in the water of River Arc, with a water column depth of 50 cm. In a clear-sky day of May in Southern France the sunlight energy reaching the ground could be equivalent to around 7 h of continuous irradiation at 30 W m^{-2} UV irradiance (Chiron et al., 2007). It is therefore possible to convert $t_{1/2}$ in days by making the hypothesis that a single day would be made up of 7 h = 2.5×10^4 s of irradiation at 30 W m^{-2} UV irradiance. Upon adoption of this approach one gets $t_{1/2} = 10$ days. This is the approximate time scale that would be required to halve the initial concentration of the complex Fe^{3+}–CLA in the water of River Arc in May. Under the hypothesis of continuous clear-sky periods, from the data of Frank and Klöpffer (1988) the corresponding time scale in February would be 2.6 times longer (around 26 days), and in November even 4 times as much (40 days).

The calculated time scale is limited compared to the residence time of water in the river Arc (1 day) where monitoring data have shown a high persistence of CLA in the water phase, in particular during winter (Feitosa-Felizzola and Chiron, 2009), but it could be significant in other cases when surface waters are exposed to sunlight for a longer period. For instance, the fraction of river water in the Rhône delta (Southern France) that is used for flooding the paddy fields has a residence time of some months in shallow fields ($d = 10$ cm) and lagoons ($d = 1$ m), before reaching the Mediterranean Sea (Chiron et al., 2007). In such a scenario the direct photolysis of Fe^{3+}–CLA would be highly significant as a removal pathway of CLA from surface waters.

It is possible to make a comparison with the expected lifetime of ROX in river water, due to reaction with $^{\bullet}OH$. For ROX it is reported $k_{\cdot OH} = 5\times10^9\ M^{-1}\,s^{-1}$ (Dodd et al., 2006), and the corresponding value for CLA is unlikely to be very different. It is possible to model the steady-state [$^{\bullet}OH$] in the surface layer of natural waters, on the basis of the water chemical composition (Chiron et al., 2007). With the River Arc data (0.15 mM NO_3^-, 25 mg L^{-1} NPOC), one gets [$^{\bullet}OH$] = 2×10^{-16} M for 30 W m^{-2} sunlight UV irradiance. In the case of ROX the half-life time would be $t_{1/2} = 0.693$ ($k_{\cdot OH}$ [$^{\bullet}OH$])$^{-1}$ = 7×10^5 s of continuous 30 W m^{-2} UV irradiation. This would correspond to around 30 days in May. Moreover, the photolysis of Fe^{3+}–CLA ($t_{1/2} = 10$ days in May) was assessed in the whole water column, and not only in the surface layer. Considering that almost complete sunlight absorption ($f_{tot} = 0.96$) takes place in the first 10 cm of water, namely one fifth of the whole column, the $t_{1/2}$ value due to $^{\bullet}OH$ should be multiplied by a factor of at least 5. A half-life time of 150 days for reaction with $^{\bullet}OH$ would just be a lower limit, because the photochemistry in the surface layer is more intense than in the first 10 cm. It can therefore be concluded that the photolysis of Fe^{3+}–ML could be a more important transformation process for macrolides than the reaction with $^{\bullet}OH$.

4. Conclusions

The phototransformation of clarithromycin and roxithromycin, two human-used macrolide (MLs) antibiotics was investigated in surface waters. Degradation in water would occur via the direct photolysis of the Fe(III)–MLs complexes. Hydroxyl radicals, singlet oxygen and other photooxidants generated from nitrate ions and from the excited chromophores present in humic acids appeared to have only a limited impact on the overall degradation of MLs. A photolysis model applied to Fe^{3+}–CLA in river water showed that a half-life of 40 days was predicted under clear-sky irradiation in November, 26 days in February, and 10 in May for clarithromycin. Direct photolysis would therefore not be able to significantly reduce the environmental concentrations of MLs in rivers, due to a too short water residence time but might be important in shallow lakes and lagoons. Photoinduced degradation of MLs mainly implied changes in the structure of the aglycone, probably leading to their detoxification because the pseudoerythromycin derivatives have very little antimicrobial activity.

Supplementary material

Supplementary material associated with this article can be found in the online version, at 10.1016/j.watres.2009.01.027.

REFERENCES

Belden, J., Maul, J., Lydy, M., 2007. Partioning and photodegradation of ciprofloxacin in aqueous system in the presence of organic matter. Chemosphere 66, 1390–1395.

Besse, J.-P., Garric, J., 2008. Human pharmaceuticals in surface waters. Implementation of a prioritization methodology and application to the French situation. Toxicol. Lett. 176, 104–123.

Boreen, A., Arnold, W., McNeill, K., 2004. Photochemical fate of sulfa drugs in the aquatic environment: sulfa drugs containing five-membered heterocyclic groups. Environ. Sci. Technol. 38, 3933–3940.

Braslavsky, S.E., 2007. Glossary of terms used in photochemistry. third edition. Pure Appl. Chem. 79, 293–465.

Calamari, D., Zuccato, E., Castiglioni, S., Bagnati, R., Fanelli, R., 2003. Strategic survey of therapeutic drugs in the rivers Po and Lambro in northern Italy. Environ. Sci. Technol. 37, 1241–1248.

Chiron, S., Minero, C., Vione, D., 2006. Photodegradation processes of the antiepileptic drug carbamazepine, relevant to estuarine waters. Environ. Sci. Technol. 40, 5977–5983.

Chiron, S., Minero, C., Vione, D., 2007. Occurrence of 2,4-dichlorophenol and of 2,4-dichloro-6-nitrophenol in the Rhône river delta (Southern France). Environ. Sci. Technol. 41, 3127–3133.

Dodd, M., Buffle, M.-A., Von Gunten, U., 2006. Oxidation of antibacterial molecules by aqueous ozone: meaty-specific reaction kinetics and application to ozone-based wastewater treatment. Environ. Sci. Technol. 40, 1969–1977.

Feitosa-Felizzola, J., Temime, B., Chiron, S., 2007. Evaluating on-line solid-phase extraction coupled to liquid chromatography-ion trap mass spectrometry for reliable quantification and confirmation of several classes of antibiotics in urban wastewaters. J. Chromatogr., A 1164, 95–104.

Feitosa-Felizzola, J., Chiron, S., 2009. Occurrence and distribution of selected human-used antibiotics in a small Mediterranean stream (Arc River, Southern France). J. Hydrol., 364, 50–57

Frank, R., Klöpffer, W., 1988. Spectral solar photon irradiance in Central Europe and the adjacent North Sea. Chemosphere 17, 985–994.

Gharbi-Benarous, J., Delaforge, M., Jankowski, C., Girault, J.P., 1991. A comparative NMR study between the macrolide antibiotic roxithromycin and erythromycin A with different biological properties. J. Med. Chem. 34, 1117–1125.

Gierczyk, B., Schroeder, G., Przybylski, P., Brzezinski, B., Bartl, F., Zundel, G., 2005. ESI MS, NMR and PM5 semiempirical studies of oligomycin A and its complexes with Li^+ and Na^+ cations. J. Mol. Struct. 738, 261–270.

Gros, M., Petrovic, M., Barcelo, D., 2007. Wastewater treatment plants as a pathway for aquatic contamination by pharmaceuticals in the Ebro river basin (Northest Spain). Environ. Toxicol. Chem. 26, 1553–1562.

Hamdan, I., 2003. Comparative in-vitro investigations of the interaction between some macrolides and Cu(II), Zn(II) and Fe(II). Pharmazie 58, 223–224.

Isidori, M., Lavorgna, M., Nardelli, A., Pascarella, L., Parrella, A., 2005. Toxic and genotoxic evaluation of six antibiotics on non-target organisms. Sci. Total Environ. 346, 87–98.

Kari, F., Giger, W., 1995. Modeling the photochemical degradation of ethylenediaminetetraacetate in the River Glatt. Environ. Sci. Technol. 29, 2814–2827.

Kim, S.C., Carlson, K., 2007. Temporal and spatial trends in the occurrence of human and veterinary antibiotics in aqueous and river sediment matrices. Environ. Sci. Technol. 41, 50–57.

Kidwage, I., Janassen, G., Busson, R., Hoogmartens, J., Vanderhaeghe, H., Verbist, L., 1987. Identification of novel erythromycin derivatives in mother liquor concentrates of *Streptomyces Erythraeus*. J. Antibiot. 40, 1–6.

Kibwage, I., Busson, R., Janssen, G., Hoogmartens, J., Vanderhaeghe, H., 1987. Translactonization in erythromycins. J. Org. Chem. 52, 990–996.

Knappe EU project, 2008. Knowledge and Need Assessment on Pharmaceutical Products in Environmental Waters. http://www.knappe-eu.org.

Leonard, S., Ferraro, M., Adams, E., Hoogmartens, J., Van Schepdael, A., 2006. Application of liquid chromatography/ion trap mass spectrometry to the characterization of the related substances of clarithromycin. Rapid Commun. Mass Spectrom. 20, 3101–3110.

Li, S., Purdy, W.C., 1992. Circular dichroism, ultraviolet, and proton nuclear magnetic resonance spectroscopic studies of the chiral recognition mechanism of β-cyclodextrin. Anal. Chem. 64, 1405–1412.

Managaki, S., Murata, A., Takada, H., Tuyen, B., Chiem, N., 2007. Distribution of macrolides, sulfonamides and trimethoprim in tropical waters: ubiquitous occurrence of veterinary antibiotics in the Mekong delta. Environ. Sci. Technol. 41, 8004–8010.

Masubuchi, Y., Horie, T., 2007. Toxicological significance of mechanism-based inactivation of cytochrome P-450 enzymes by drugs. Critical Rev. Toxicol. 37, 389–412.

McArdell, C., Molnar, R., Suter, M., Giger, W., 2003. Occurrence and fate of macrolide antibiotics in wastewater treatment plants and in the Glatt valley watershed. Switzerland Environ. Sci. Technol. 37, 5479–5486.

Miao, X.-S., Bischay, P., Chen, M., Metcalfe, C., 2004. Occurrence of antibacterials in the final effluents of wastewater treatment plants in Canada. Environ. Sci. Technol. 38, 3533–3541.

Pal, S., 2006. A journey across the sequential development of macrolides and ketolides related to erythromycin. Tetrahedron 62, 3171–3200.

Pei, R., Cha, J., Carlson, K., Pruden, A., 2007. Response of antibiotic resistance genes (ARG) to biological treatment in dairy lagoon water. Environ. Sci. Technol. 41, 5108–5113.

Pham, A.N., Waite, T.D., 2008. Oxygenation of Fe(II) in natural waters revisited: kinetic modeling approaches, rate constant estimation and the importance of various reaction pathways. Geochim. Cosmochim. Acta 72, 3616–3630.

Schlünzen, F., Zarivach, R., Harms, J., Bashan, A., Tocilj, A., Albrecht, R., Yonath, A., Franceschi, F., 2001. Structural basis for the interaction of antibiotics with the peptidyl transferase centre in eubacteria. Nature 413, 814–821.

Sibley, S., Pedersen, J., 2008. Interaction of the macrolide antimicrobial clarithromycin with dissolved humic acid. Environ. Sci. Technol. 42, 422–428.

Werner, J., Arnold, W., McNeill, K., 2006. Water hardness as a photochemical parameter: tetracycline photolysis as a function of calcium concentration, magnesium concentration and pH. Environ. Sci. Technol. 40, 7236–7241.

Werner, J., Chintapalli, M., Lundeen, R., Wammer, K., Arnold, W., McNeill, K., 2007. Environmental photochemistry of tylosin: effective, reversible photoisomerization to a less active isomer, followed by photolysis. J. Agric. Food Chem. 55, 7062–7068.

Wong-Wah-Chung, P., Mailhot, G., Aguer, J.-P., Bolte, M., 2006. Fate of a stylbene-type fluorescent agent (DSBP) in the presence of Fe(III) aquacomplexes: From the redox process to the photodegradation. Chemosphere 65, 2185–2192.

Xue, H., Sigg, L., Kari, F., 1995. Speciation of EDTA in natural waters: exchange kinetics of Fe–EDTA in river water. Environ. Sci. Technol. 29, 59–68.

Ye, Z., Weinberg, H., Meyer, M., 2007. Trace analysis of trimethoprim and sulfonamide, macrolide, quinolone and tetracycline antibiotics in chlorated drinking water using liquid chromatography electrospray tandem mass spectrometry. Anal. Chem. 79, 1135–1144.